Icarus 206 (2010) 64–73

Contents lists available at ScienceDirect

Icarus

journal homepage: www.elsevier.com/locate/icarus

Global distribution, structure, and solar wind control of low altitude current sheets at Mars

J.S. Halekas *, D.A. Brain

Space Sciences Laboratory, University of California, 7 Gauss Way, Berkeley, CA 94720, USA

ARTICLE INFO

Article history:
Received 21 August 2008
Revised 29 November 2008
Accepted 22 December 2008
Available online 7 January 2009

Keywords:
Mars
Magnetospheres
Ionospheres

ABSTRACT

We present the results of the first systematic survey of current sheets encountered by Mars Global Surveyor in its ∼400 km mapping orbit. We utilize an automated procedure to identify over 10,000 current sheet crossings during the ∼8 year mapping mission. The majority of these lie on the night side and in the polar regions, but we also observe over 1800 current sheets at solar zenith angle <60°. The distribution and orientation of current sheets and their dependence on solar wind drivers suggests that most magnetotail current sheets have a local induced magnetospheric origin caused by magnetic field draping. On the other hand, most current sheets observed on the day side likely result from solar wind discontinuities advected through the martian system. However, the clustering of low altitude dayside current sheet crossings around the perimeters of strongly magnetized crustal regions, and the smaller than expected rotations in the IMF draping direction, suggest that crustal magnetic fields may also play an indirect role in their formation. The apparent thicknesses of martian current sheets, and the characteristics of electrons observed in and around the current sheets, suggest one of two possibilities. Martian current sheets at low altitudes are either stationary, with thicknesses of a few hundred km and currents carried by low energy (<10 eV) electrons, or they move at tens of km/s, with thicknesses of a few thousand km and currents carried by ions.

1. Introduction

The flowing plasma of the solar wind interacts directly with the atmosphere of Mars, producing an induced magnetosphere. At Earth and many other planets, an intrinsic magnetic field produced by a core dynamo provides the primary obstacle to solar wind flow. However, at Mars, much like at Venus and comets, the primary obstacle to the solar wind flow consists of plasma of planetary origin – ionized atmospheric and exospheric gases (Cloutier et al., 1999; Nagy et al., 2004). Mars' unique remanent crustal magnetic fields do perturb the interaction with the solar wind (Mitchell et al., 2001; Crider et al., 2002; Brain et al., 2005), but the martian magnetosphere still closely resembles that of Venus.

The magnetic field morphology at Mars is generally well-approximated by a gasdynamic model of plasma flow (Spreiter and Stahara, 1992; Crider et al., 2004). Magnetic field lines fail to completely penetrate the conducting ionosphere, and drape around the effective obstacle, resulting in locally near-horizontal field draping on the day side, with field lines swept back into a two-lobed magnetotail extending in the flow direction on the night side (Crider et al., 2004). Draped field lines can eventually diffuse through the ionosphere, but most field lines instead advect with the plasma as it flows around the ionospheric obstacle. As at Venus, plasma flow around the ionosphere results in velocity shear which can cause a characteristic field draping toward the sub-solar point often termed "weathervaning" – in essence, magnetic field lines are dragged through the ionosphere and stretched in an anti-solar direction as they slip around the obstacle (Cloutier et al., 1999; Brain et al., 2006a). These magnetic field draping characteristics prevail mainly below the magnetic pileup boundary (MPB), with more disordered fields observed in the magnetosheath outside of the MPB (Bertucci et al., 2003).

Like the terrestrial magnetotail, the martian magnetotail consists of two lobes of oppositely directed magnetic field, with a central current sheet separating them. However, at Mars, draped fields rather than intrinsic dynamo fields form the two lobes, and the upstream interplanetary magnetic field (IMF) rather than the dynamo axis controls the orientation of the lobes and current sheet. Phobos 2 first observed the martian magnetotail current sheet, with a thickness of ∼1000 km, at 2.86 R_M in the tail, and confirmed its control by the upstream IMF (Riedler et al., 1991; Yeroshenko et al., 1990). Surprisingly, Mars Global Surveyor (MGS) observations showed that the general two-lobed structure of the magnetotail, including the central current sheet, manifests itself even at ∼400 km altitudes (Ferguson et al., 2005). Further study of current sheets encountered

* Corresponding author. Fax: +1 510 643 8302.
E-mail address: jazzman@ssl.berkeley.edu (J.S. Halekas).

0019-1035/$ - see front matter © 2009 Elsevier Inc. All rights reserved.
doi:10.1016/j.icarus.2008.12.032

by MGS revealed frequent current sheet crossings even at low altitudes on the night side (in the magnetotail), occurring above all but the strongest crustal field regions (Halekas et al., 2006). The magnetotail current sheet has an orientation roughly consistent with the magnetic field configuration expected from draped magnetic fields in an induced magnetosphere (controlled by IMF direction), but solar wind conditions and the relative position of crustal magnetic fields also appear to affect its structure and location on the night side.

Previous MGS observations of magnetic field draping patterns on the day side also show magnetic field signatures which indicate the existence of significant current systems in the ionosphere and at the MPB (Bertucci et al., 2003; Cloutier et al., 1999). However, these current systems only produce a rotation in the magnetic field, rather than a full reversal. MGS has also observed field-aligned currents associated with auroral-like processes (Brain et al., 2006b; Halekas et al., 2008), presumably caused by accelerated electrons. However, we only observe these features in regions of strong crustal magnetic fields, where the currents (though strong) produce only small relative perturbations in the magnetic field. Outside of the magnetotail, no one has reported observations of magnetospheric current sheets strong enough to produce a magnetic field reversal. However, no one has previously performed a systematic study of current sheets in the entire martian system.

Current sheets in the martian magnetosphere present an interesting area of study, with relevance to a number of fundamental space physics processes. Plasma measurements from both Phobos 2 and Mars Express (MEX) have revealed significant populations of accelerated cold planetary ions in or near the central magnetotail current sheet (i.e. the plasmasheet) (Lundin et al., 1989; Rosenbauer, 1989; Federov et al., 2006, 2008). Magnetotail ion acceleration has been variously ascribed to non-adiabatic transport (Ip, 1992), magnetic tension forces (Lichtenegger et al., 1995; Dubinin et al., 1993a,b), and pickup processes (Luhmann, 1990). More recently, MEX observations imply a controlling role for the convection electric field in energizing plasmasheet ions (Federov et al., 2006, 2008).

In addition, MGS has also observed electron acceleration in some current sheet crossings (primarily a subset confined to localized regions) (Halekas et al., 2006). It has been suggested that this electron acceleration may result from magnetic field reconnection which drives tailward transport and energization of photoelectrons from the dayside (Uluşen and Linscott, 2008). Another recent study (Eastwood et al., 2008) has also found signatures suggestive of reconnection occurring in the martian magnetotail, lending credence to an important role for reconnection. However, auroral-like processes (Lundin et al., 2006; Brain et al., 2006b) also accelerate both electrons and ions in the magnetotail. Some of these "auroral" events may be related to magnetotail current sheet crossings, as suggested by a recent statistical study of auroral-like electron spectra observed by MGS (Halekas et al., 2008).

In this paper, we further investigate the distribution, structure, and solar wind control of current sheets encountered by MGS at its ~400 km mapping altitude in the martian magnetosphere. Our previous study (Halekas et al., 2006) employed an exhaustive "by hand" search of only one martian year of data, and was limited to current sheets observed on the night side (in the magnetotail) and aligned with the magnetotail axis. In this study, we cast a much wider net by utilizing an automated search over the entire ~8 years of MGS mapping data, from both the night side and day side, in order to characterize current sheets of all orientations at low altitude throughout the martian system.

2. Mars Global Surveyor data and proxies

The work described in this paper primarily utilizes data from the MGS Magnetometer and Electron Reflectometer (MAG/ER) instrument (Acuña et al., 2001; Mitchell et al., 2001). The MAG consisted of two identical fluxgate magnetometers, which provided fast vector measurements (up to 32 samples/s) of magnetic fields. The ER was a symmetric hemispherical "top-hat" electrostatic analyzer, which measured the energy and angular distributions of 10 eV to 20 keV electrons. It sampled electron fluxes at thirty logarithmically spaced energy channels, in sixteen $22.5^\circ \times 14^\circ$ sectors, which span the entire $360^\circ \times 14^\circ$ field of view.

We organize our results by solar wind parameters, as derived from proxy measurements. Magnetic field draping direction and sub-solar magnetic field strength are derived from dayside MAG data above weakly or non-magnetized regions, once per orbit (Brain et al., 2005, 2006a). We use these quantities as proxies for upstream IMF clock angle and solar wind dynamic pressure. These proxies have been shown to organize measurements of martian field structure and topology, plasma boundary locations, escaping ion fluxes, and auroral-like electron distributions (see review by Brain et al., 2007)).

3. Identifying current sheet crossings

In a previous study (Halekas et al., 2006), we surveyed current sheet crossings by MGS during one martian year in the magnetotail, as identified "by hand". In the current study, we opted instead to utilize an automated procedure to identify current sheet crossings throughout the martian magnetosphere, over the entire MGS mapping mission. We developed the algorithm for this procedure based on the results of the previous study in order to quickly, simply, and reliably identify current sheet crossings.

In our previous study, we searched for current sheet crossings in all regions, including those with strong crustal fields. We found very few in areas with crustal fields, possibly because any current sheets are pushed to higher altitudes over these regions. Given the lack of observations of current sheets in these regions, and the difficulty of reliably identifying current sheet crossings in an automated fashion over regions with strong crustal fields, in this study we only search for current sheets in regions where the Cain model (Cain et al., 2003) predicts crustal field magnitudes <20 nT at orbital altitude. Also, in our previous study, we found that virtually all current sheet crossings at low altitudes occur relatively quickly. Therefore, we use an algorithm optimized to identify current sheet crossings of a few hundred seconds or less. Though this limits our search to relatively thin current sheets, we have surveyed enough orbits to rule out any significant identifiable population of thicker current sheets. Finally, in our previous study, we found that current sheet identification is only reliable for sufficiently large induced magnetic field strengths. Therefore, we only search for current sheet crossings with average non-crustal (induced) field magnitudes (estimated roughly by subtracting the Cain model crustal field from the measured field) on each side of the current sheet >7.5 nT.

Our algorithm, which essentially finds magnetic minima separating regions with nearly anti-parallel magnetic fields, proceeds as follows. For each time, we calculate the average magnetic field vector from a window extending from 150 s beforehand to 45 s beforehand, and that from 45 s after to 150 s after the time of interest. We calculate the dot product between these two vectors (normalized) in order to search for magnetic field reversals. When the dot product between these vectors is less than -0.7 (i.e. a rotation $>134^\circ$) and the magnetic field magnitude is less than 75% of the average in the surrounding 300 s window (excluding 150 s around the time of interest), we tentatively identify a current sheet crossing. If this crossing lasts for 12 s or more (thus excluding data errors or gaps, as well as features associated with waves/turbulence), we positively identify a current sheet crossing. In Figs. 1 and 2, we show two current sheets identified by the algorithm

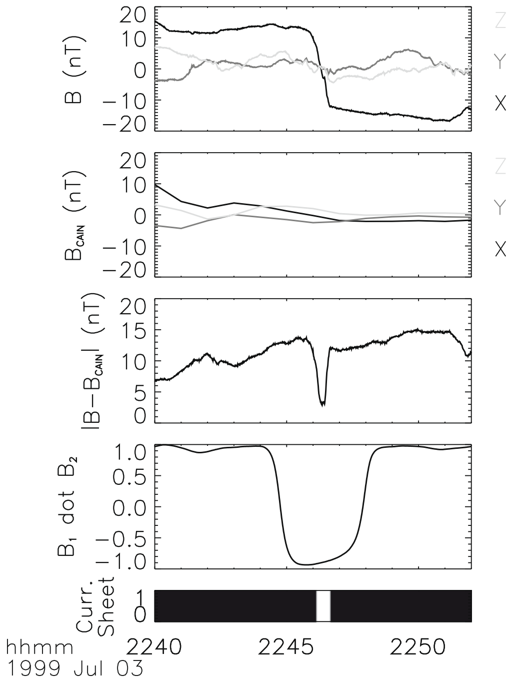

Fig. 1. Nightside current sheet crossing at 22:46 UT on 1999/07/03, at a solar zenith angle (SZA) of 132° and an MSO position of [−0.745, −0.194, −0.794] R_M. Panels show magnetic field in MSO coordinates, Cain model predictions of crustal fields, estimated magnitude of non-crustal fields, and the dot product of the average normalized magnetic field vector from an appropriate window (described in text) before the observation time with that after the observation time. Black and white bar shows (in white) where an automated procedure found a current sheet.

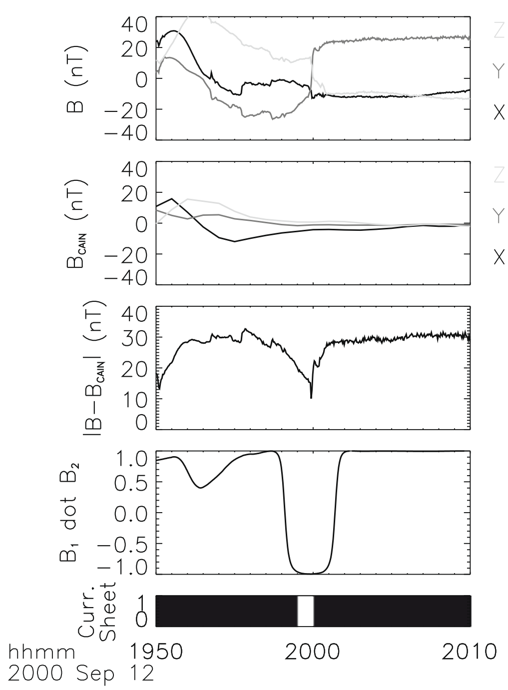

Fig. 2. Dayside current sheet crossing at 20:00 UT on 2000/09/12, at SZA = 27° and MSO position of [0.997, 0.477, −0.155] R_M. All panels same as in Fig. 1.

described above, demonstrating the quantities used by the algorithm to positively identify current sheet crossings.

Though this algorithm is relatively simple in concept and execution, we have found by extensive testing over hundreds of orbits that it reliably identifies current sheet crossings with any orientation, not only in the magnetotail region previously investigated, but also in other regions of the martian magnetosphere. Thus, we can build up a data base of low altitude current sheet crossings throughout the martian system, extending over the ∼8 years of the MGS mapping mission. This large data base, of over 10,000 current sheet crossings, allows us to investigate the global distribution, structure, and solar wind control of current sheets at low altitudes in the martian magnetosphere.

4. Current sheet orientation

A critical question is: How do current sheets observed at low altitudes in the martian magnetosphere form and evolve? Most nightside current sheets likely form as a result of anti-parallel magnetic field draping in the magnetotail, as described above (Halekas et al., 2006). However, current sheets in the polar regions and day side, and perhaps some night side current sheets, could instead represent solar wind discontinuities advected and amplified in the martian system. In addition, some current sheets may form as the IMF interacts directly or indirectly with crustal magnetic fields. It will prove difficult to differentiate between these various possibilities utilizing single-spacecraft observations. We must rely largely on statistical studies of current sheet parameters to determine the prevailing mechanism for current sheet formation.

We first consider the orientation of the observed current sheets. In Fig. 3, we sketch several possible origins for current sheets encountered by MGS on the day side and night side of Mars. On the night side, current sheets could form as a result of anti-parallel magnetic field draping (i.e. an induced current sheet, Fig. 3d) or as a result of IMF discontinuities in the solar wind advected through the martian system (Fig. 3b). In the first case (induced origin), we require highly draped magnetic fields, in order to form a current sheet at ∼400 km altitude on the night side. In the second case (solar wind origin), we require significant compression/amplification of typical solar wind magnetic fields in order for our automated procedure to detect the current sheet (the typical IMF strength outside of the martian system is ∼3–4 nT, well below our threshold). In addition, a solar wind current sheet would have to remain at least locally stable as it advected around the planet, undergoing compression and distortion. On the day side, meanwhile, current sheets could similarly represent discontinuities in the solar wind (Fig. 3a), or could instead form as a result of exaggerated magnetic field draping and weathervaning (Cloutier et al., 1999; Brain et al., 2006a), with magnetic field lines forming an extended loop temporarily anchored in the ionosphere (Fig. 3c). In the first case (solar wind origin), the same considerations as above hold, though an IMF current sheet need not advect as far for us to observe it on the day side. In the second case (induced origin), seemingly only significant velocity shear and differential flow could create such an extended loop of magnetic field.

In addition to the two possibilities considered above, crustal magnetic fields could have an influence on the formation and evolution of current sheets. Anti-parallel draping of the IMF over a crustal magnetic field region could directly form a current sheet (Fig. 3e), or an existing solar wind current sheet could be compressed and amplified over a crustal magnetic field region (Fig. 3f). Both of these possibilities likely occur in the martian system; however, our study of MGS mapping data, which does not identify current sheets directly over strong crustal field regions or at high altitudes, may not be capable of addressing either of these situations.

In order to determine current sheet orientations, we use the well-known minimum variance analysis (MVA) technique introduced by Sonnerup and Cahill (1967). While this technique relies on a number of assumptions, including local planarity and stationarity, it has proven itself as a useful technique in space plasma physics, subject to careful interpretation. As an illustrative exam-

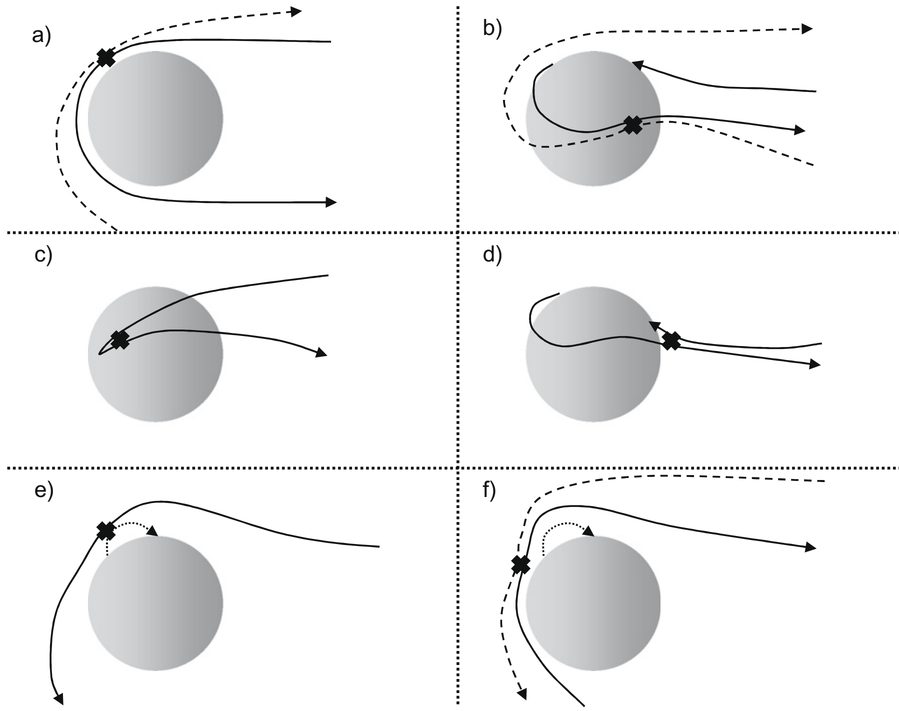

Fig. 3. Possible magnetic field orientations for current sheets of solar wind (a, b) and induced magnetospheric (c, d) origin, on the day side (a, c) and night side (b, d). In addition, two possible scenarios for crustal field influence on current sheets, including direct formation by draping over a crustal field (e), and compression of an existing current sheet by draping over a crustal field (f).

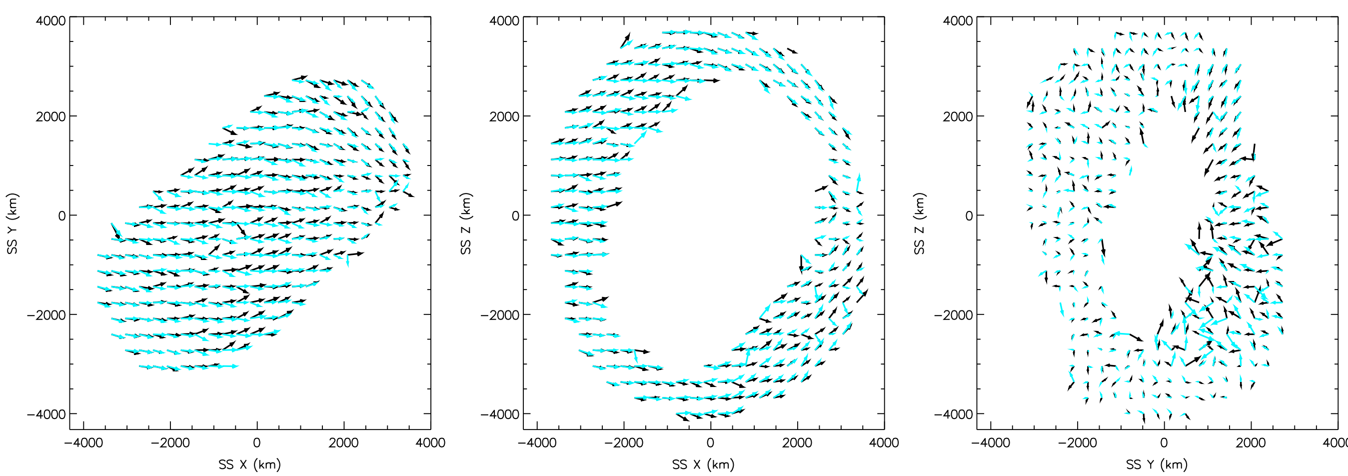

Fig. 4. Average maximum variance direction (current sheet axis) for 4993 current sheet crossings with well-characterized eigenvectors, projected in MSO *X–Y*, *X–Z*, and *Y–Z* planes, in blue. For comparison, the average magnetic field draping direction for 5009 randomly selected mapping observations over locations with crustal field magnitudes <5 nT at orbital altitude, in black. For both sets of observations, we normalized the vectors to unit length, with their *X*-components >0. This removes the effect of the IMF draping polarity and the ambiguity in the direction of the current sheet axes, allowing a direct comparison of all data simultaneously. (For interpretation of the references to color in this figure legend, the reader is referred to the web version of this article.)

ple, we apply this technique to the two example current sheets shown in Figs. 1 and 2. Both of these current sheet crossings have very well-constrained MVA properties, with the ratio of first and second eigenvalues $\lambda_1/\lambda_2 > 40$, and the ratio of second and third eigenvalues $\lambda_2/\lambda_3 > 10$. The night side example (Fig. 1) has a maximum variance eigenvector (corresponding to the current sheet axis) of $e_1 = [0.98, -0.15, -0.11]$ and a minimum variance eigenvector (corresponding to the current sheet normal) of $e_3 = [0.15, -0.99, -0.02]$. As expected for an induced magnetotail current sheet formed by magnetic field draping, the current sheet axis lies along the Mars–Sun line. Meanwhile, its normal lies nearly in the ecliptic, consistent with an induced current sheet corresponding to the average IMF orientation near the ecliptic. The day side example (Fig. 2), on the other hand, has $e_1 = [0.22, -0.89, 0.41]$ and $e_3 = [0.88, 0.35, 0.30]$. In this case, the current sheet axis lies almost tangential to the planet, with its normal almost radial. A nearly radial current sheet normal supports a solar wind origin, since in the induced weathervaning case one would expect the current sheet normal to instead lie almost parallel to the surface, rather than radial.

These examples suggest that induced current sheets might prove more common on the night side, and solar wind current sheets on the day side. However, we can investigate the average properties of a much larger subset of current sheet crossings observed by MGS in order to address this question more thoroughly. We elect to consider all current sheets where an MVA analysis

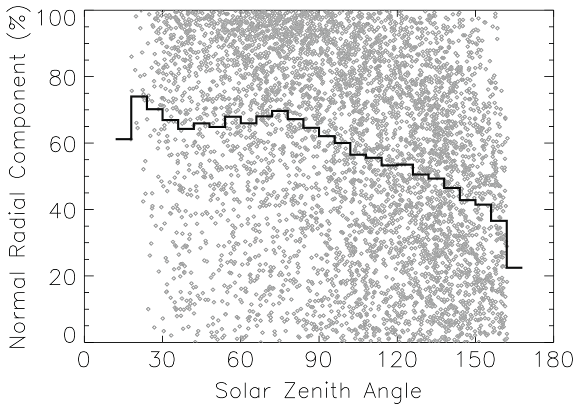

Fig. 5. Radial component of minimum variance direction (current sheet normal) for 4993 current sheet crossings with well-characterized eigenvectors, as a function of SZA. Thick black trace shows average minimum variance radial component for each SZA bin.

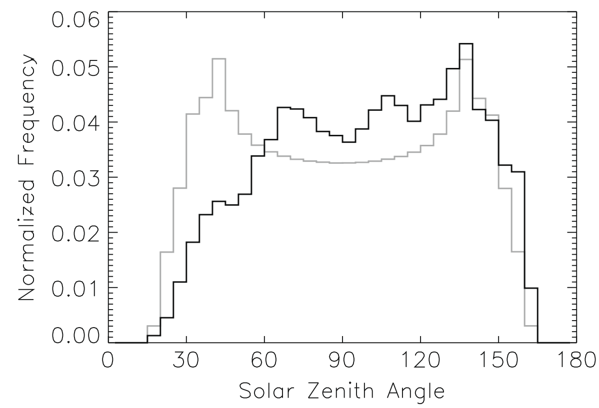

Fig. 6. Normalized SZA occurrence frequency distribution for 10,812 current sheet crossings (black) compared with overall SZA coverage of MGS mapping orbit (gray).

gives even marginal results, in order to maximize our sample size. Specifically, we pick all current sheets for which $\lambda_1/\lambda_2 > 4$, and $\lambda_2/\lambda_3 > 4$, implying reasonably constrained current sheet normals and axes, but not to a high degree of accuracy. In Fig. 4, we plot the current sheet axes thus determined as an averaged vector field, in three orthogonal projections. For comparison, we plot a random sample of averaged magnetic field vectors, sampled outside of significant crustal field regions, in order to outline the average induced magnetospheric field draping pattern. We find that the average current sheet axes compare consistently with the average field draping pattern. Minor differences do exist; for instance, current sheet axes on the night side and in the polar regions tend to align more closely with the Mars–Sun line then the average draping pattern, suggesting a more heavily draped configuration, where the two extended tail lobes dominate the nightside magnetic field signature even at 400 km altitude. This observation appears consistent with the hypothesis that mostnight side current sheets have an induced magnetospheric origin. On the day side, meanwhile, we find no coherent difference between the average current sheet axes and the average magnetic field direction, implying that no special draping configuration prevails when current sheets form on the day side, consistent with a solar wind origin rather than one involving an extremely weathervaned draping configuration. We note that the disordered current sheet axes and average field vectors in the dayside southern hemisphere may result from interactions with the strong crustal magnetic fields mainly located in the southern hemisphere.

As a final check on the average current sheet orientation, in Fig. 5 we plot the radial component of the current sheet normal for the same subset of current sheet crossings, as a function of solar zenith angle (SZA). We find that current sheet normals on the day side tend to have a large radial component, consistent with a solar wind origin, and seemingly inconsistent with an induced magnetospheric weathervaning configuration. In the polar regions and on the night side, on the other hand, current sheet normals tend to have a more radial orientation at low SZA and a less radial orientation at high SZA, consistent with current sheets aligned with the Mars–Sun axis. Though these general trends prevail, some mixture of current sheet orientations remains apparent at all SZA.

Given the apparent prevalence of current sheets of solar wind origin on the day side of Mars, we find it intriguing to speculate on what factors may control their dynamics. As a solar wind current sheet advects through the martian system, the magnetic field lines on either side of the current sheet will be subject to the same plasma interactions and velocity shears which act to create the induced magnetosphere magnetic field draping pattern (discussed in Section 1). As magnetic field lines on each side of the current sheet distort and drape around the ionospheric obstacle and/or around crustal magnetic fields, the current sheet structure may not remain stable and coherent. Instead, reconnection may take place in these current sheets as they interact with local plasma and distort in response to magnetic tension and stress. As solar wind current sheets interact with ionospheric plasma and crustal magnetic structures, they may form extremely complicated magnetic field structures, potentially including multi-point reconnection and intricate flux ropes. Without a full simulation of these processes, we cannot answer address these questions definitively.

5. Current sheet distribution

We now consider the spatial distribution of current sheet crossings observed by MGS at mapping altitude. Rather than limiting ourselves only to those current sheets with well-defined orientations (from MVA analysis) as above, we instead consider the entire set of current sheets identified by our automated procedure, thereby nearly doubling our data set. We show the SZA distribution of these current sheet crossings in Fig. 6, demonstrating that MGS encounters current sheets at all SZA, but relatively more often in the polar regions and night side than on the day side. We display the locations of these same current sheet crossings in geographic coordinates in Fig. 7, plotted over a map of crustal field magnitude at orbital altitude as predicted from the Cain model (Cain et al., 2003). We separate current sheet crossings into three different SZA ranges, in order to look at differences in crossing locations for dayside, polar region, and nightside current sheets. Due to the fixed 2 am/2 pm orbit of MGS, there are no data points at mid-latitudes (±25°) in the middle (polar region) SZA range. In addition, there are fewer data points at latitudes >35° in the other two SZA ranges, because MGS can only reach these regions at these SZA in certain seasons.

We find widely distributed dayside crossings, but with some clustering near the periphery of crustal magnetic field regions, suggesting that IMF interaction with crustal magnetic fields may play some role in compressing and amplifying IMF current sheets (as in Fig. 3f), or perhaps even creating new current sheets (as in Fig. 3e). We investigated these dayside current sheet crossings near the periphery of strong crustal magnetic field regions in more detail, in order to try to ascertain if either of these possible scenarios might explain this clustering. We show a typical current sheet crossing in this region in Fig. 8. This figure clearly shows that we do not observe the current sheet at the boundary of the crustal field region and the draped IMF. Instead, the current

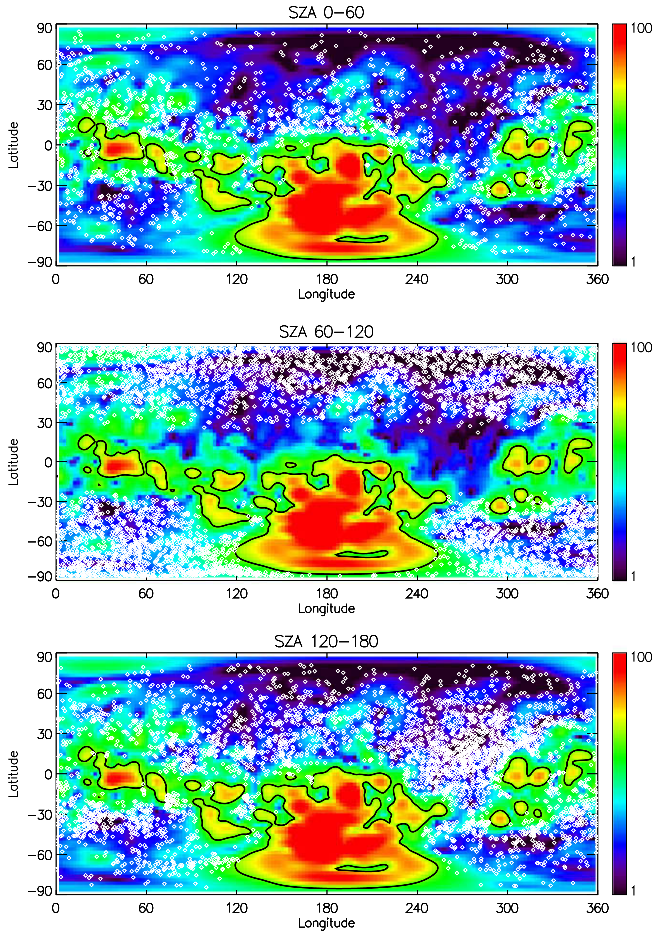

Fig. 7. Locations of current sheet crossings in geographic coordinates (shown in white), for three SZA ranges (1834 crossings for SZA < 60, 5229 for 60 < SZA < 120, 3749 for SZA > 120). Due to the fixed 2 am/2 pm orbit of MGS, some geographical locations are unattainable in the middle SZA range. Colors show crustal field magnitude from Cain model, with black contour indicating 20 nT level.

sheet is slightly offset from the periphery of the crustal field region, and the anti-parallel magnetic fields which form the current sheet are not the crustal field and the IMF, but two non-crustal field components. For nearly every such current sheet crossing that we have investigated, this general picture holds true, implying that we almost never observe current sheets formed directly by IMF draping over crustal fields. This physical situation likely does occur at Mars; however, it likely only takes place directly over strong crustal field regions and/or at higher altitudes (neither of which our data set covers). On the other hand, crustal fields may still affect the formation of the current sheet, perhaps by compressing and amplifying an existing solar wind current sheet as it drapes over the crustal field region, as suggested in Fig. 3f.

In the polar regions, meanwhile, we find nearly randomly distributed current sheet crossings at high latitudes (the fixed 2 am/2 pm orbit of MGS ensures that it does not reach equatorial latitudes for this SZA range), implying little control by crustal magnetic fields. Finally, on the night side, MGS encounters current sheets most frequently at equatorial latitudes, in regions with weak or no crustal magnetic fields. This distribution is consistent with an induced magnetospheric origin, since we should observe the current sheet location at low altitude most often over regions with weak or no crustal fields, where crustal fields cannot push draped magnetic fields and the current sheet region higher in altitude.

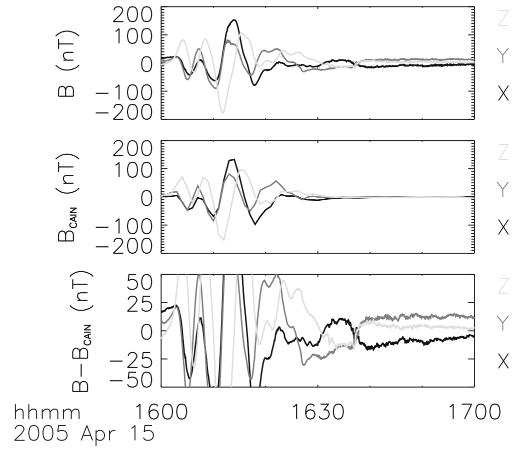

Fig. 8. Typical current sheet crossing on the day side near a region with strong crustal magnetic fields, observed at 16:37 UT on 2005/04/15, at SZA = 50°, geographic longitude and latitude of [161°, 22°], and MSO position of [0.716, 0.430, 0.746] R_M. Panels show measured magnetic field, Cain model field, and residuals in MSO coordinates.

As noted by Halekas et al. (2006), nightside current sheet crossing location appears to depend to some degree on solar wind drivers, suggesting additional effects associated with crustal magnetic location and orientation. For some nightside current sheets, this apparent control may result from reconnection between the IMF and crustal fields, as proposed by Uluşen and Linscott (2008). However, this mechanism may dominate, or may instead only operate for a small subset of nightside current sheets, in a few favored locations with optimal crustal magnetic field geometry.

6. Dependence on external drivers

In order to understand the behavior and formation of current sheets in the martian magnetosphere, we wish to determine how the solar wind drives the system. Absent an upstream monitor, this proves difficult. However, as described in Section 2, we can use dayside magnetic field measurements to construct proxies for several relevant solar wind parameters. By leveraging these proxies, we can obtain some idea of how the martian system responds to upstream conditions.

We first consider the effect of the upstream IMF clock angle. In order to address this parameter, we use a magnetic field draping proxy, defined by Brain et al. (2006a) in terms of angles between the observed dayside magnetic field direction (at high northern latitude) and local east. These provide at best an unsatisfactory proxy, since we can only indirectly relate this low altitude field direction to the upstream IMF clock angle. However, this proxy at least provides us some information about the relative magnetic field draping configuration. In Fig. 9, we show frequency distributions for the IMF draping proxy (azimuth and elevation angles) during current sheet crossings, separated into three SZA ranges, and compared to the overall distribution for the entire MGS mapping mission. Given the large number of observations presented in these histograms, even small differences are statistically significant. Chi-square tests show that all of the distributions presented in this figure are different to a level such that there is less than a 10^{-8} chance that they are drawn from the same distribution. As noted by Brain et al. (2006a), the average magnetic field draping azimuth distribution clusters into two peaks, which likely correspond to the two Parker spiral directions. Meanwhile, the average elevation angle distribution clusters near zero, corresponding to the nearly horizontally draped magnetic fields on the day side. We find that the draping proxy distributions for current sheet crossings do not dif-

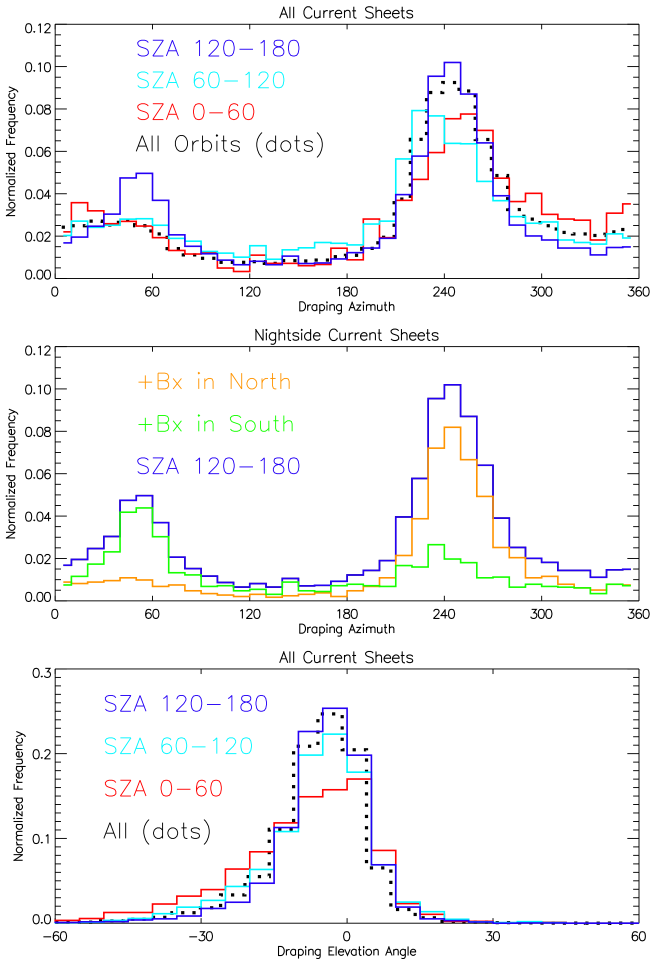

Fig. 9. Normalized draping azimuth (top two panels) and elevation angle (bottom panel) occurrence frequency distributions for current sheet crossings in three SZA ranges (1834 crossings for SZA < 60, 5229 for 60 < SZA < 120, 3749 for SZA > 120), compared with distributions for the entire MGS mapping orbit duration. Middle panel shows only nightside crossings, with separate plots for crossings with positive $B_x > 5$ nT in the north (1658) and those with positive $B_x > 5$ nT in the south (1328).

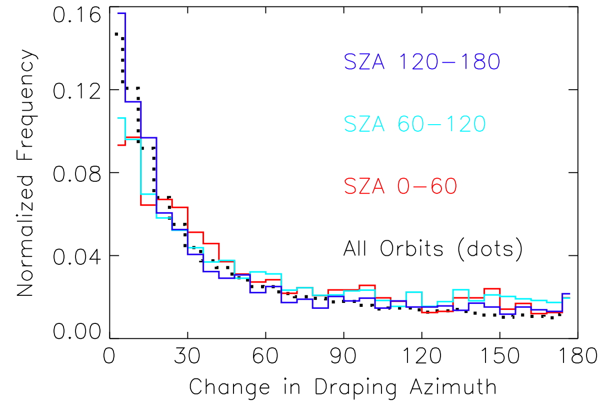

Fig. 10. Normalized occurrence frequency distribution of the change in draping azimuth from one orbit to the next for current sheet crossings in three SZA ranges (1834 crossings for SZA < 60, 5229 for 60 < SZA < 120, 3749 for SZA > 120), compared with distribution for the entire MGS mapping orbit duration.

fer greatly from these average distributions for the entire mission (though they are statistically significantly different), showing that IMF conditions when MGS encounters current sheets do not radically differ from those when it does not. However, we do note some differences. First, when we observe current sheets on the day side, magnetic field draping does not cluster as tightly in azimuth, and trends more locally downward in elevation angle (less tangential to the surface). Meanwhile, we observe current sheets on the nightside slightly more often than average for northeastward draping, but otherwise we cannot easily visually distinguish the night side distribution from the overall average. Distributions for polar current sheets in general lie intermediate between day side and nightside distributions.

As perhaps the best currently available test of the induced nature of nightside current sheets, we repeat an exercise devised by Halekas et al. (2006), utilizing a larger data set. In the middle panel of Fig. 9, we again show the draping azimuth distribution for times when MGS encounters current sheets on the night side, and separate it into two components. One component consists of current sheets for which MGS encounters the sunward tail lobe (i.e. that where the magnetic field direction points sunward) in the north and the tailward lobe in the south, and the other when the sunward tail lobe lies in the south and the tailward lobe in the north. These two components prove well-separated by magnetic field draping proxy, in the sense expected for an induced magnetotail current sheet. For southward draping (180–360° azimuth) on the day side, the sunward lobe tends to lie in the north, and for northward draping (0–180° azimuth) on the day side, the sunward lobe tends to lie in the south. We find that this separation does not perfectly characterize the two distributions, but given the local, inexact, variable nature of the draping proxy, it proves impressively consistent.

In addition to considering the draping proxy for each orbit, we can examine the change in the draping proxy from orbit-to-orbit. If we encounter a current sheet of solar wind origin in the martian system, we would expect a significant difference between the IMF clock angle before the current sheet crossing and that after. For an induced current sheet crossing produced inside the magnetosphere, on the other hand, one would expect no more change than average. In Fig. 10 we plot the distribution of the orbit-to-orbit change in the draping azimuth proxy for three SZA ranges, as compared to the overall distribution for the entire MGS mapping mission. For nightside current sheet crossings, we find a distribution nearly identical to that for the whole mission (though still significantly different, with only a 3×10^{-6} chance of being drawn from the same distribution), consistent with an induced origin for these magnetotail current sheets. On the other hand, for current sheet crossings on the day side and polar regions, we find a ∼40% smaller probability for changes in draping azimuth of less than 30°. The distributions for day side and polar crossings are statistically nearly the same, but both very statistically different from that for the whole mission or the night side, with less than a 10^{-8} chance that they are drawn from the same distribution. This represents a significant effect, consistent with IMF changes affecting the likelihood of observing current sheets on the day side or polar regions. However, we find it surprising that MGS does not observe an even more pronounced effect. One might expect to observe a much larger than 30° rotation in draping azimuth associated with most current sheets of solar wind origin. Either small rotations in IMF suffice to produce current sheets on the martian dayside, larger rotations exist but do not persist on orbital time scales, or (contrary to other evidence) most of the day side current sheets actually have an induced magnetospheric or crustal field origin.

We next consider the effects of upstream solar wind dynamic pressure. Again, we cannot observe this parameter directly; however, by measuring dayside magnetic field strengths (away from crustal fields) and fitting to a theoretical curve, we determine the

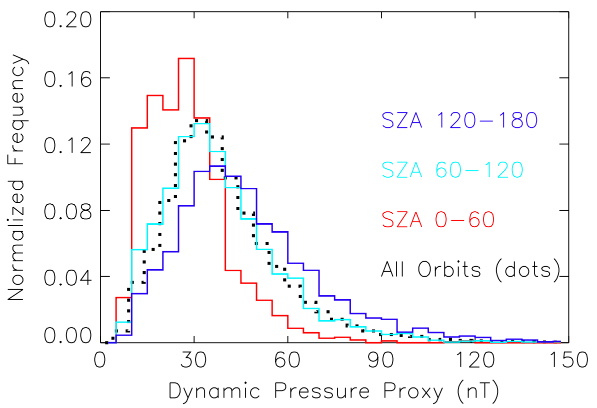

Fig. 11. Normalized solar wind dynamic pressure proxy occurrence frequency distribution for current sheet crossings in three SZA ranges (1834 crossings for SZA < 60, 5229 for 60 < SZA < 120, 3749 for SZA > 120), compared with distribution for the entire MGS mapping orbit duration.

sub-solar magnetic field strength, which we assume linearly related to the solar wind dynamic pressure (in the absence of crustal magnetic fields and ionospheric interactions; Brain et al., 2005). We plot frequency distributions of this parameter in Fig. 11 for current sheet crossings in three SZA ranges, and compare to the average distribution for the entire MGS mapping mission. We find clear and significant differences in dynamic pressure proxy measurements when MGS encounters current sheets (all distributions significantly different to a level better than 10^{-8}). When we observe current sheet crossings on the day side, we infer much lower than average dynamic pressures. Meanwhile, when MGS crosses current sheets on the night side, we infer higher than average dynamic pressures. Though clearly significant, the reasons for these effects remain obscure. A helpful reviewer suggested that the high dynamic pressures observed for nightside crossings might result from a systematic bias stemming from our selection criterion of $B > 7.5$ nT; however, this does not appear to be the case, as distributions of dynamic pressure for random times selected with the same criterion show no systematic bias.

We suggest that higher dynamic pressures (which compress the martian magnetosphere) should enhance magnetic field draping, making it easier for the tail lobes and central current sheet to form at low altitudes in the magnetotail and thus easier for MGS to observe the current sheet on the night side at its mapping altitude of ~400 km. Meanwhile, the association of low dynamic pressures with dayside current sheets remains a mystery, but we offer a few suggestions. Low dynamic pressures allow the martian magnetospheric interaction to expand. This would make it more likely for MGS to lie below the MPB, and would also make it more likely for MGS to lie in a region significantly influenced by crustal magnetic fields. Absent any other clear mechanism, we suggest that one or both of these factors may affect the likelihood of observing current sheets on the day side.

7. Current sheet properties

We now investigate the properties of individual current sheet crossings, in order to try to constrain what species carries the current in these current sheets. We first fit the magnetic field magnitude across each current sheet crossing to a Harris current sheet model of the form $B(t) = A\tanh(|t - t_0|/W) + B_0$, with A the amplitude, W the half-width, B_0 the minimum magnetic field, and t_0 the time at which we cross the center of the current sheet. We then calculate the crossing time as twice the half-width, or $2W$. We can also use the MVA determinations of normal directions to convert this to the time to cross the current sheet at normal incidence. We plot distributions of the crossing time and the crossing time at normal incidence, for current sheets in three SZA ranges, in Fig. 12. We find that it takes <100 s (well within our identification time window) to cross most current sheets (assuming normal incidence), and the distributions for the three SZA ranges differ very little, other than a slightly longer average crossing time for night side current sheet crossings (even this small difference is statistically significant, with less than a 10^{-8} chance that the nightside distribution is taken from the same distribution as the other two, which are statistically nearly the same). Taken at face value, these results imply very thin current sheets with thicknesses of a few hundred km or less (given the MGS orbital velocity of ~3.37 km/s). However, this conclusion only remains valid for locally stationary current sheets. If the current sheets themselves move, their speed could greatly exceed that of the spacecraft, implying a much greater true thickness for the current sheets. Absent multi-point measurements, we cannot determine which holds true. We can, however, consider two end-member cases.

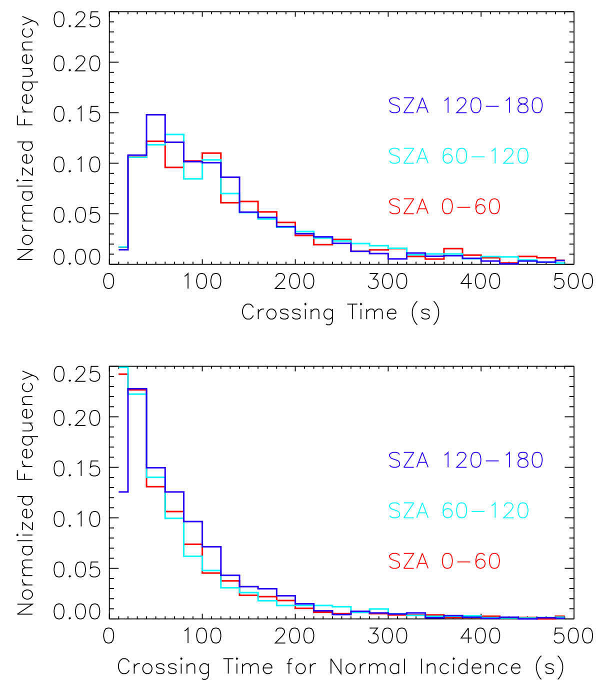

Fig. 12. Normalized occurrence frequency distributions of the time to cross the current sheet (top panel) and the crossing time corrected to assume normal incidence (bottom panel), for current sheet crossings with well-determined eigenvectors, in three SZA ranges (772 crossings for SZA < 60, 2342 for 60 < SZA < 120, 1879 for SZA > 120).

If none of the current sheets we observe move at significant speeds, then they have a true thickness of a few hundred km or smaller. This conclusion appears surprising, given typical proton inertial lengths and gyroradii on the order of a few hundred to a few thousand km, suggesting likely current sheet thicknesses of a few thousand km (more in line with observations from Phobos 2 at higher altitude in the magnetotail; Riedler et al., 1991; Yeroshenko et al., 1990). As discussed in Halekas et al. (2006), low energy electrons might instead carry the current in these current sheets.

If, on the other hand, current sheets actually have thicknesses of a few thousand km, then this would imply current sheet speeds on the order of several tens of km/s. These speeds do not seem unreasonable, given typical solar wind speeds of ~400 km/s (though at ~400 km altitude we should observe much smaller flow speeds). However, the fact that we observe little difference in crossing time distributions for different SZA ranges would imply

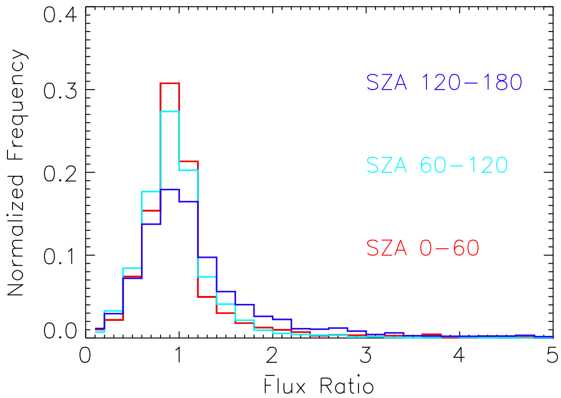

Fig. 13. Normalized occurrence frequency distribution of the ratio of electron flux at 115 eV at 90° pitch angle in the current sheet region to that in the surrounding plasma for current sheet crossings in three SZA ranges (1834 crossings for SZA < 60, 5229 for 60 < SZA < 120, 3749 for SZA > 120).

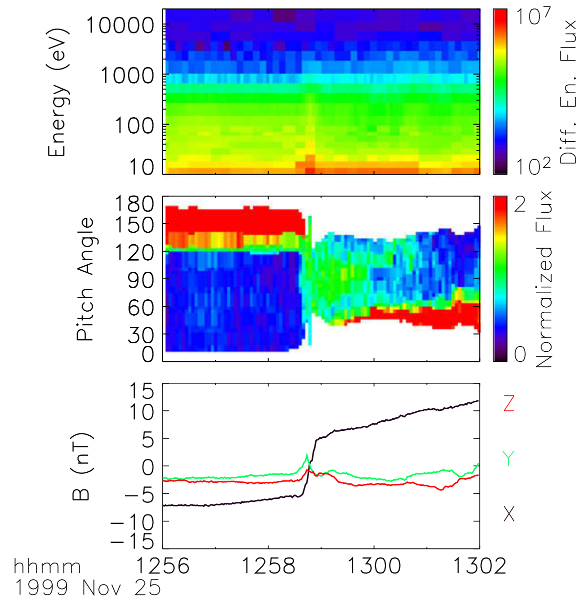

Fig. 14. Nightside current sheet crossing at 12:59 UT on 1999/11/25, with electron differential energy flux as a function of energy and time, normalized electron flux distribution as a function of pitch angle and time, and magnetic field components in MSO coordinates.

that current sheets move at nearly the same speed in all regions of the martian magnetosphere, which seems unlikely. In addition, if current sheets actually move at these speeds in the magnetotail, than the current sheets observed by Phobos 2 deeper in the magnetotail must have had even greater true thicknesses, or moved less rapidly. Therefore, neither interpretation proves entirely satisfactory.

We can also investigate the properties of electrons in and around the current sheets. As a simple check, we calculate the average electron flux at 115 eV at 90° pitch angle within the central current sheet (i.e., for $|t - t_0| < W$, using the model discussed above), and compare it to the average flux outside of the central current sheet, but within 120 s on either side of the current sheet. We show distributions of the ratio of flux within the current sheet to that outside, for three SZA ranges, in Fig. 13. We find a distribution centered on unity, implying no consistent enhancement in electron flux in the current sheets. By only considering 90° pitch angle, we avoid any effects of the changing field of view of the MGS ER instrument (since 90° pitch angle is always in the field of view); however, this conclusion holds up when considering any range of pitch angles and/or energies. The distribution for nightside current sheets has a slight (statistically significant) tail at positive values, showing a small population of nightside current sheets with an increase in electron flux. This population consists mainly of current sheets within a unique region discussed in detail by Brain et al. (2006b), Halekas et al. (2006, 2008), and Uluşen and Linscott (2008), and may result from reconnection and acceleration of electrons, possibly photoelectrons from the dayside. Other than these special cases, we find no consistent increase in electron flux within current sheets. This conclusion appears robust over the energy range of the MGS ER, from tens of eV to tens of keV. Thus, if electrons carry the current in these current sheets, they must lie at a few eV (as suggested by Halekas et al., 2006) or at very high energies.

In the end, we cannot make any strong conclusions about the current carrier in current sheets observed at low altitude in the martian magnetosphere, especially absent any coordinated measurements of electrons, ions, and magnetic fields (since MGS lacks ion measurements, and MEX lacks magnetic field measurements). In the future, investigators might successfully address this problem using two-spacecraft conjunctions. For now, we suggest that the data provide slightly stronger evidence for ions as the current carrier at least in the magnetotail, given terrestrial experience and MEX observations of accelerated ions in the martian magnetotail plasmasheet region. If so, this would imply that magnetotail current sheets likely have true thicknesses of a few thousand km, and move at tens of km/s. For dayside current sheets, on the other hand, we can draw no substantive conclusions whatsoever. However, given the similarity in the distributions of apparent thicknesses and electron properties, they may have the same current carriers as those on the night side. This would imply that dayside current sheets should also have accelerated ion populations, and should also have true thicknesses of a few thousand km, and speeds of tens of km/s. However, we cannot answer this question without full plasma and magnetic field measurements, utilizing either spacecraft conjunctions or measurements from a future mission.

8. Unusual current sheet crossings

As a final item of interest, we note an unusual type of current sheet revealed in our investigation, which should prove worthy of further investigation. In Fig. 14, we show a current sheet observed on the night side. We observe a very typical magnetic field profile, comparable to most magnetotail current sheets. However, we see very unique electron angular distributions, which show field-aligned electrons traveling in opposite directions along the magnetic field (but both towards Mars) on opposite sides of the current sheet. We commonly observe field-aligned electrons in the martian magnetosphere. Solar wind electrons often prove anisotropic, especially the strahl component, and can preserve this anisotropy as they move from the solar wind into the magnetosphere. Investigators have used this property in the past in order to trace magnetic field topology (Dubinin et al., 1993b). However, anisotropic solar wind electrons almost always travel mainly in one direction along the magnetic field. Bidirectional streaming can occur in the solar wind, but generally only in association with closed magnetic field structures like magnetic clouds, or upstream from shocks (Gosling, 1990; Gosling et al., 1993). We can tentatively rule out both of these possibilities by looking at dayside magnetic field data. Therefore, we suggest that the field-aligned electrons here may result from fundamental physical processes taking place in the current sheet. For instance, a reconnection event (perhaps like that discussed by Eastwood et al. (2008)) downstream from MGS could produce field-aligned electrons traveling towards Mars on both sides of the current sheet, as we observe here. We have observed over a hundred examples of this phenomenon, primarily in the central magnetotail. A detailed study of these events lies beyond the scope of this paper, but promises to reveal potentially interesting physics of the martian magnetotail current sheet.

9. Conclusions

We have conducted the first systematic survey of current sheets encountered by MGS during its mapping orbit. This work extends a previous study (Halekas et al., 2006)—which only looked at current sheets aligned with the Mars–Sun line, and only on the night side in the magnetotail—by using a newly developed automated procedure to identify current sheet crossings with any orientation on the day side, polar regions, and night side at mapping altitude of ∼400 km. We identified over 10,000 current sheet crossings during the ∼8 year MGS mapping mission. The majority of these lie on the nightside and in the polar regions, but we observe some current sheets even at very small SZA. The distribution and orientation of current sheets and their dependence on solar wind drivers suggests that most magnetotail current sheets have a local induced magnetospheric origin, while most day side current sheets result from IMF discontinuities advected through the martian system. However, the clustering of dayside current sheet crossings around crustal magnetic field locations, and the smaller than expected IMF rotations, suggest that crustal magnetic fields may also play an indirect role in the formation of current sheets on the day side. The apparent thicknesses of martian current sheets, and the characteristics of electrons observed in and around the current sheets, suggest one of two possibilities. martian current sheets either have thicknesses of a few hundred km (stationary), with currents carried by low energy (<10 eV) electrons, or they have thicknesses of a few thousand km (and move at tens of km/s), with currents carried by ions. Martian current sheet structures will likely prove rich in terms of fundamental physics processes, with a strong potential for reconnection both in current sheets of solar wind origin as they advect around the ionosphere and interact with crustal magnetic fields and in the induced magnetotail as plasma fills in the wake, sweeping draped magnetic field lines towards each other.

Acknowledgments

This work was supported by NASA Grant NNG05GJ24G. We thank Tielong Zhang for a useful discussion which greatly improved this work. We thank two reviewers for helpful and constructive comments which significantly strengthened this manuscript.

References

Acuña, M.H., and 13 colleagues, 2001. Magnetic field of Mars: Summary of results from the aerobraking and mapping orbits, J. Geophys. Res., 106, 23403–23418.

Bertucci, C., Mazelle, C., Acuña, M.H., Russell, C.T., Slavin, J.A., 2003. Magnetic field draping enhancement at the Martian magnetic pileup boundary from Mars Global Surveyor observations. Geophys. Res. Lett. 30. doi:10.1029/2002GL015713.

Brain, D.A., Halekas, J.S., Lillis, R.J., Mitchell, D.L., Lin, R.P., Crider, D.H., 2005. Variability of the altitude of the Martian sheath. Geophys. Res. Lett. 32. doi:10.1029/2005GL023126. L18203.

Brain, D.A., Mitchell, D.L., Halekas, J.S., 2006a. The magnetic field draping direction at Mars from April 1999 through August 2004. Icarus 182, 464–473.

Brain, D.A., Halekas, J.S., Peticolas, L.M., Lin, R.P., Luhmann, J.G., Mitchell, D.L., Delory, G.T., Bougher, S.W., Acuña, M.H., Reme, H., 2006b. On the origin of aurorae at Mars. Geophys. Res. Lett. 33. doi:10.1029/2005GL024782. L01201.

Brain, D.A., 2007. Mars Global Surveyor measurements of the martian solar wind interaction. Space Sci. Rev. 126, 77–112.

Cain, J.C., Ferguson, B.B., Mozzoni, D., 2003. An $n = 90$ internal potential function of the martian crustal magnetic field. J. Geophys. Res. 108. doi:10.1029/2000JE001487. 5008.

Cloutier, P.A., and 19 colleagues, 1999. Venus-like interaction of the solar wind with Mars. Geophys. Res. Lett. 26, 2685–2688.

Crider, D.H., and 12 colleagues, 2002. Observations of the latitude dependence of the location of the martian magnetic pileup boundary. Geophys. Res. Lett. 29, 1170. doi:10.1029/2001GL013860.

Crider, D.H., Brain, D.A., Acuña, M.H., Vignes, D., Mazelle, C., Bertucci, C., 2004. Mars Global Surveyor observations of solar wind magnetic field draping around Mars. Space Sci. Rev. 111, 203–221.

Dubinin, E., Lundin, R., Norberg, O., Pissarenko, N., 1993a. Ion acceleration in the Martian tail: Phobos observations. J. Geophys. Res. 98, 3991–3997.

Dubinin, E., Lundin, R., Schwingenschuh, K., 1993b. Solar wind electrons as tracers of the Martian magnetotail topology. J. Geophys. Res. 99, 21233–21240.

Eastwood, J.P., Brain, D.A., Halekas, J.S., Drake, J.S., Phan, T.D., Oieroset, M., Mitchell, D.L., Lin, R.P., Acuña, M.H., 2008. Evidence for collision less magnetic reconnection at Mars. Geophys. Res. Lett. 35, L02106. doi:10.1029/2007GL032289.

Federov, A., and 44 colleagues, 2006. Structure of the Martian wake. Icarus 182, 329–336. doi:10.1016/j.icarus.2005.09.021.

Federov, A., and 49 colleagues, 2008. Comparative analysis of Venus and Mars magnetotails. Planet. Space Sci. 56, 812–817.

Ferguson, B., Cain, J.C., Crider, D.H., Harnett, E., Brain, D.A., 2005. External fields on the night-side of Mars at Mars Global Surveyor mapping altitudes. Geophys. Res. Lett. 32. doi:10.1029/2004GL021964. L161095.

Gosling, J.T., 1990. Coronal mass ejections and magnetic flux ropes in interplanetary space. In: Russell, C.T., Priest, E.R., Lee, L.C. (Eds.), Physics of Magnetic Flux Ropes, Geophys. Monograph, vol. 58. AGU, p. 343.

Gosling, J.T., Bame, S.J., Feldman, W.C., McComas, D.J., Phillips, J.L., Goldstein, B.E., 1993. Counterstreaming suprathermal electron events upstream of corotating shocks in the solar wind beyond 2 AU, Ulysses. Geophys. Res. Lett. 20, 2335.

Halekas, J.S., Brain, D.A., Lillis, R.J., Fillingim, M.O., Mitchell, D.L., Lin, R.P., 2006. Current sheets at low altitudes in the martian magnetotail. Geophys. Res. Lett. 33. doi:10.1029/2006GL026229. L13101.

Halekas, J.S., Brain, D.A., Lin, R.P., Luhmann, J.G., Mitchell, D.L., 2008. Distribution and variability of accelerated electrons at Mars. Adv. Space Res. 41, 1347–1352.

Ip, W.-H., 1992. Ion acceleration at the current sheet of the martian magnetosphere. Geophys. Res. Lett. 19, 2095–2098.

Lichtenegger, H., Schwingenschuh, K., Dubinin, E., Lundin, R., 1995. Particle simulation in the Martian magnetotail. J. Geophys. Res. 100, 21659–21667.

Luhmann, J.G., 1990. A model of the ion wake of Mars. Geophys. Res. Lett. 17, 869–872.

Lundin, R., Borg, H., Hultqvist, B., Zakharov, A., Pellinen, R., 1989. First measurements of the ionospheric plasma escape from Mars. Nature 341, 609–612.

Lundin, R., and 22 colleagues, 2006. Plasma acceleration above Martian magnetic anomalies. Science 311, 980–983.

Mitchell, D.L., Lin, R.P., Mazelle, C., Reme, H., Cloutier, P.A., Connerney, J.E.P., Acuña, M.H., Ness, N.F., 2001. Probing Mars' crustal magnetic field and ionosphere with the MGS electron reflectometer. J. Geophys. Res. 106, 23419–23427.

Nagy, A.F., and 14 colleagues, 2004. The plasma environment of Mars. Space Sci. Rev. 111, 33.

Rosenbauer, H., Shutte, N., Galeev, A., Gringauz, K., Apathy, I., 1989. Ions of Martian origin and plasma sheet in the Martian magnetosphere: Initial results of the TAUS experiment. Nature 341, 612.

Riedler, W., Schwingenschuh, K., Lichtenegger, H., Mohlman, D., Rustenbach, J., Yeroshenko, Ye., Achache, J., Slavin, J., Luhmann, J.G., Russell, C.T., 1991. Interaction of the solar wind with the planet Mars: Phobos 2 magnetic field observations. Planet. Space Sci. 39, 75–81.

Sonnerup, B.U.Ö., Cahill Jr., L.J., 1967. Magnetopause structure and attitude from Explorer 12 observations. J. Geophys. Res. 72, 171–183.

Spreiter, J.R., Stahara, S.S., 1992. In: Luhmann, J.G., Tatrallyay, M., Pepin, R.O. (Eds.), Computer Modeling of the Solar Wind Interaction with Venus and Mars, Venus and Mars: Atmospheres, Ionospheres, and Solar Wind interactions, Geophysical Monograph 66, 345–383.

Uluşen, D., Linscott, I., 2008. Low-energy electron current in the martian tail due to reconnection of draped interplanetary magnetic field and crustal magnetic fields. J. Geophys. Res. 113. E06001.

Yeroshenko, Y., Riedler, W., Schwingenschuh, KI., Luhmann, J.G., Ong, M., Russell, C.T., 1990. The magnetotail of Mars: Phobos observations. Geophys. Res. Lett. 17, 885–888.